Manufacturing and investigation of barium oxide thin films for photodetector applications

A. A. Salih, H. M. Ali, R. H. Athab, B. H. Hussein*
Department of Physics, College of Education for Pure Science / Ibn Al-Haitham, University of Baghdad, Baghdad, Iraq

Barium oxide was made in this work using an easy and affordable chemical technique. FTIR, AFM UV-visible, and X-ray diffraction (XRD) are used to describe the produced samples. The tetragonal phase of BaO nanoparticles with an average crystallite size of 46.5 nm was verified by X-ray diffraction experiments. The particle size was determined to be between 40 and 201 nm using the AFM micrograph. It was discovered that the BaO nanoparticles optical band gap was 4.6 eV. The sample's presence of Ba-O vibration was detected by FTIR spectra. Regarding the Operation of (Ag/BaO/Si/Ag), photodetector studied the effect of changing the molar concentration (M) for barium oxide (1M, 0.5M and 0.25M). The properties of the applied photodetector were studied, by the responsivity (Rλ) of all photodetectors. The higher responsivity was about 0.18A/W, the Specific Detectivity (D*) was 2.5×10^{12} and Quantum Efficiency (η) 49% at 0.5M for wavelength 450nm.

(Received March 12, 2024; Accepted June 20, 2024)

Keywords: Barium oxide, Nanoparticles, Crystalline size, Chemical method, Photodetector

1. Introduction

According to their numerous application based on size and design, nanotechnology and nanoscience disclose an important place from Fundamentals to Practical Implementation material research [1], where a group of atoms joined by a structural radius of less than 100 nm is regarded as a nanoparticle. The intriguing features of metal and metal oxide nanoparticles, which rely on size, shape, composition, morphology, and crystalline phase, are caused by their high surface area and high atom fraction [2, 3]. In general, the microstructure of the nanoparticles—which includes surface morphology, grain boundaries, and crystal defects—has a substantial impact on the physical properties of the particles. Consequently, learning about the microstructure of BaO-NPs is crucial to comprehending their size-dependent physical properties [3–9]. Transition metal oxide nanomaterial iron, copper, titanium, zinc, and barium oxide (BaO), among others—are considered one of the richest families of nanomaterials due to their broad range of applications and size-dependent material properties in comparison to their bulk phases. Photovoltaic sensors, high-temperature superconductors, actuators, environmental sciences, capacitors, health sciences, solar cells, Li-ion batteries, and many more sectors are among the many applications for which they are used. The white, hygroscopic, nonflammable chemical barium oxide (BaO) is. It is utilized in crown glass, cathode ray tubes, and catalysts. It has a cubic structure. Additionally, because of its large band gap (4.4 eV), barium oxide (BaO) is a highly conductive n-type semiconductor of special relevance [10–18]. Barium oxide nanoparticles are fascinating because they are used in coating, crown glass manufacturing, and catalytic applications. There are barium oxide nanoparticles in the phase structure of tetragonal crystals. Thus far, a number of methods have been established for the manufacture of BaO Nanoparticles (BaO-NPs) in order to products nanomaterials by varying shapes and sizes. These methods include thermal decomposition, sonochemical, sol–gel, chemical technique, microwave irradiation, hydrothermal, and quick-precipitation. However, these processes are expensive, poisonous, and require a lot of energy, high pressure, challenging separation, and perhaps dangerous conditions [19]. The purpose of this work is to prepare and explore the characteristics of barium oxide, followed by an examination of the

* Corresponding author: boshra.h.h@ihcoedu.uobaghdad.edu.iq
https://doi.org/10.15251/DJNB.2024.192.981

impact of varying molarity concentrations on photodetector performance. Semiconductor devices called photodetectors use electrical processes to detect optical signals. The requirement for a fast and sensitive photodetector has increased due to the wavelength extension of both coherent and incoherent light sources into the ultraviolet and far-infrared regions. Strict specifications including minimal noise, fast response times, and high sensitivity at operational wavelengths must be met by the photodetector [10]. These days, both fundamental and applied research heavily relies on the usage of thin films of semiconducting materials.

2. Preparation of samples

Sodium hydroxide (NaOH) and barium nitrate [$Ba(NO_3)_2$] are the basic materials used to create BaO-NPs chemically. The low temperature, low cost of production and ease of synthesis, make the simple chemical pathway very useful in wide industries. However, there is a drawback to this method: the finished solution contains salts, which must be removed by repeatedly washing it with distilled water. A typical preparation involved dissolving 2.4 grams of Barium nitrate (Ba(NO3)2) dissolved in 100 milliliters of deionized water (H2O) and continually stirring the mixture with a magnetic stirrer for about 15 minutes, until the Ba(NO3)2 had completely gone into solution. About 6 ml of the premade NaOH solution were added drop-wise with constant stirring for about an hour, the reaction generates a white-colored liquid. The produced mixture was retained for enabling the precipitation of all constituent particles. To remove salts from the sample, the precipitated material underwent multiple washes and centrifugations using distilled water and alcohol. In order to confirm that the precipitate had fully transformed into BaO, it was next calcined and dried at 300°C for two hours in the air. Figure 1 depicts the schematic of the synthesis process.

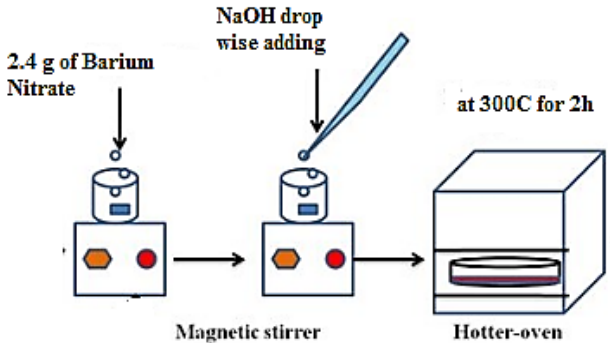

Fig. 1. Schematic of the synthesis BaONPs.

3. Result and discussion

The best method for determination the size of the crystallites is X-ray diffraction. Where the Scherrer equation [20] is used to determine the size of the produced barium oxide nanoparticles. The XRD patterns of the prepared sample of barium oxide nanoparticles are shown in fig.2 in the 2θ range 20–50°. Peaks corresponding to different planes of BaO are clearly discernible as (200), (101), (111), (310), (211) and (301), The obtained diffraction patterns are in accordance with the tetragonal phase of BaO-NPs and align well with the data provided in the "JCPDS" card No. 26-0178. This observation is further corroborated by the findings reported in the literature [2,8,21-22]. Sharp and intense peaks at 24.8,29.1 and 31.6 the synthesized nanoparticles exhibit a remarkable degree of crystallinity, demonstrating their well-defined and ordered atomic arrangement [23-25]. The crystalline size was (46.5)nm. Table1display results X-ray diffraction of barium oxide.

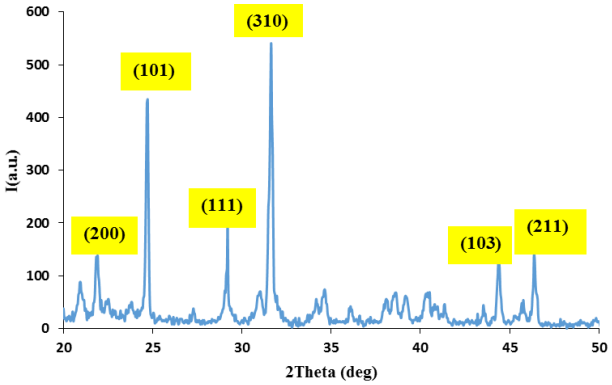

Fig. 2. XRD analysis of BaO powder.

Table 1. Symmetry of XRD of BaO.

2Theta (deg)	FWHM (deg)	hkl	Crystalline size (nm)
21.9	**0.12**	**200**	**76.6**
24.6	**0.17**	**101**	**47.9**
29.2	**0.22**	**111**	**38.8**
31.6	**0.21**	**310**	**39.4**
44.4	**0.26**	**103**	**33.0**
46.4	**0.16**	**211**	**54.1**

Surface morphology is an important parameter to identify the surface quality of the film and inside growth morphology [26]. Surface morphology of BaO nanostructure film investigated by AFM and shown in Fig. 3. The BaO film deposited shows surface roughness (root mean squared (RMS) roughness 8.09 nm). It notices that the grains are distributed in different size, as appear in Gaussian distribution, where average grain size 201 nm. The large grains are result of small grains gathering to form peaks with height of up to 98 nm and the small grains with height less than 10 nm.

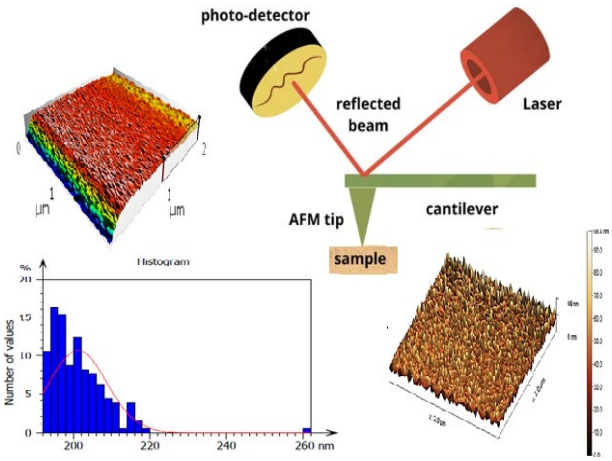

Fig. 3. AFM image of Ba-oxide thin film.

The transmittance and reflectance spectra of BaO thin films are shown in Figure 4. We examine T% and R% spectra in three different primary spectral regions to clarify how the optical behavior of as-prepared thin films is dependent on these parameters. An absorption edge is visible

in the high-energy region (E =4.1 eV or λ= 298 nm) of the BaO NPs thin film. Thin films show very little absorption in the visible range and high transparency (T% > 90%). The optical band gap of the BaO films is calculated using Tauc's expression [27,28], the BaO NPs Tauc's plot is displayed in Figure 5. It is discovered that the band gap energy for bulk phase of BaO, at 4.4 electron Volt, is lower than that of the nanophase BaO, or 4.65 eV. The principal source of this increase in optical band gap energy is the widely recognized quantum size effect of materials in the nanophase. When the particle size approaches the de Broglie wavelength of a charge carrier, typically in the nanometer range, unique quantum effects become evident., does this theory—the quantum size effect—apply [1, 29].

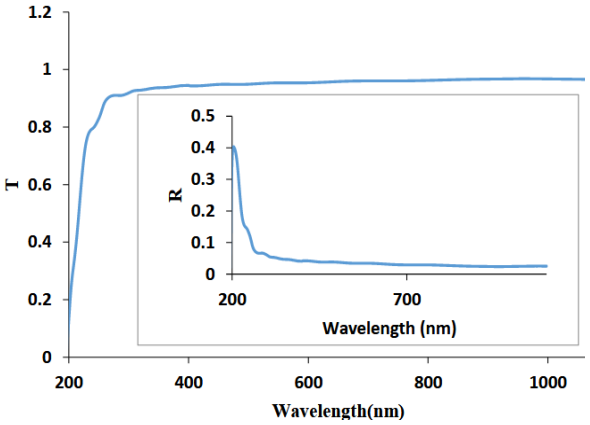

Fig. 4. Shows transmission spectra of Ba oxide spectrum.

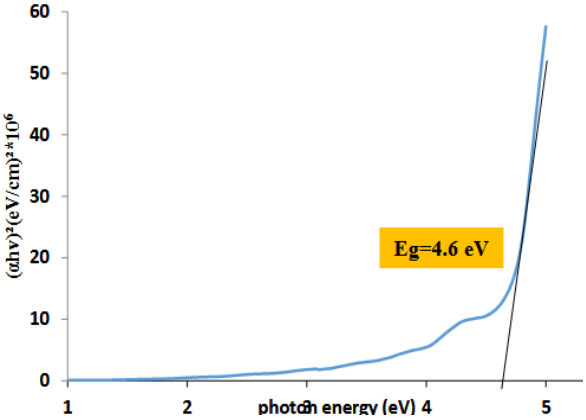

Fig. 5. A graph displaying the energy band gap of sample.

The chemical composition of the synthesized BaO-NPs was evaluated using Fourier Transform Infrared (FTIR) spectroscopy in the wavenumber range of 4000 to 400 cm-1. as shown in Figure 6. The FTIR spectrum represents a strong absorption band at ~692 cm^{-1} which corresponds to the Ba–O bond formation. In the FTIR spectra, two absorption bands are observed at approximately 1641 cm−1 and 3456 cm−1. These bands correspond to the stretching and bending vibrations of the O–H bond, respectively. [30-32]. The presence of the barium oxide bond confirms the results of XRD.

The responsivity of Ag/BaO/Si/Ag photodetectors with three different molarity concentration (1M, 0.5M and 0.25M) under the illumination as shown in Figure (7a,b and c) the wavelength in range 350-1000 nm. It observed from figures that there are two peaks in spectrum at 450nm and 850 nm, which indicted to the absorption edge of barium oxide and silicon substrate respectively. The peak at 450 nm indicted to thin film of BaO absorption. Where BaO thin film absorb incident light at this wavelength, but after increasing the wavelength the film becomes transparent, so we notice decrease in the spectral responsivity.

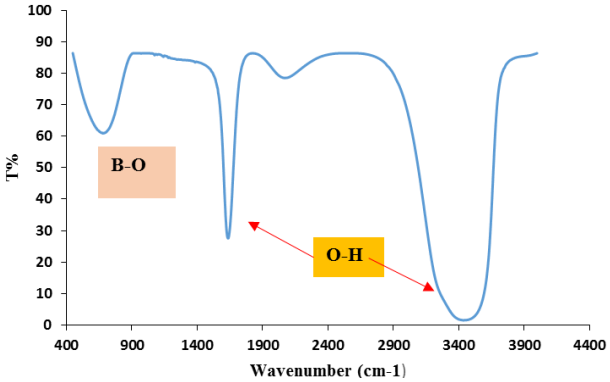

Fig. 6. FT-IR spectra of Ba oxide nanoparticles.

We also notice that spectral responsivity at wavelength >850 nm due to cut-off wavelength of Si. The device exhibit the highest responsivity value (0.10, 0.18 and 0.13A/W) at 450 nm. The Ag/BaO/Si/Ag photodetector exhibits optimal sensitivity in the near-infrared spectrum (0.38, 0.51 and 38 A/W) at 850 nm. the spectral responsivity at low molarity concentration (0.5M and 0.25M) is the higher than high molarity concentration (1M), this may be attributed to agglomeration of material at high concentration and act as defects that reduce the responsivity. The responsivity calculated from equation (1) [33,34].

$$R = I_{ph}/P_{in}\,(A/W) \tag{1}$$

where: I_{Ph} = Photocurrent, P_{in} = input power

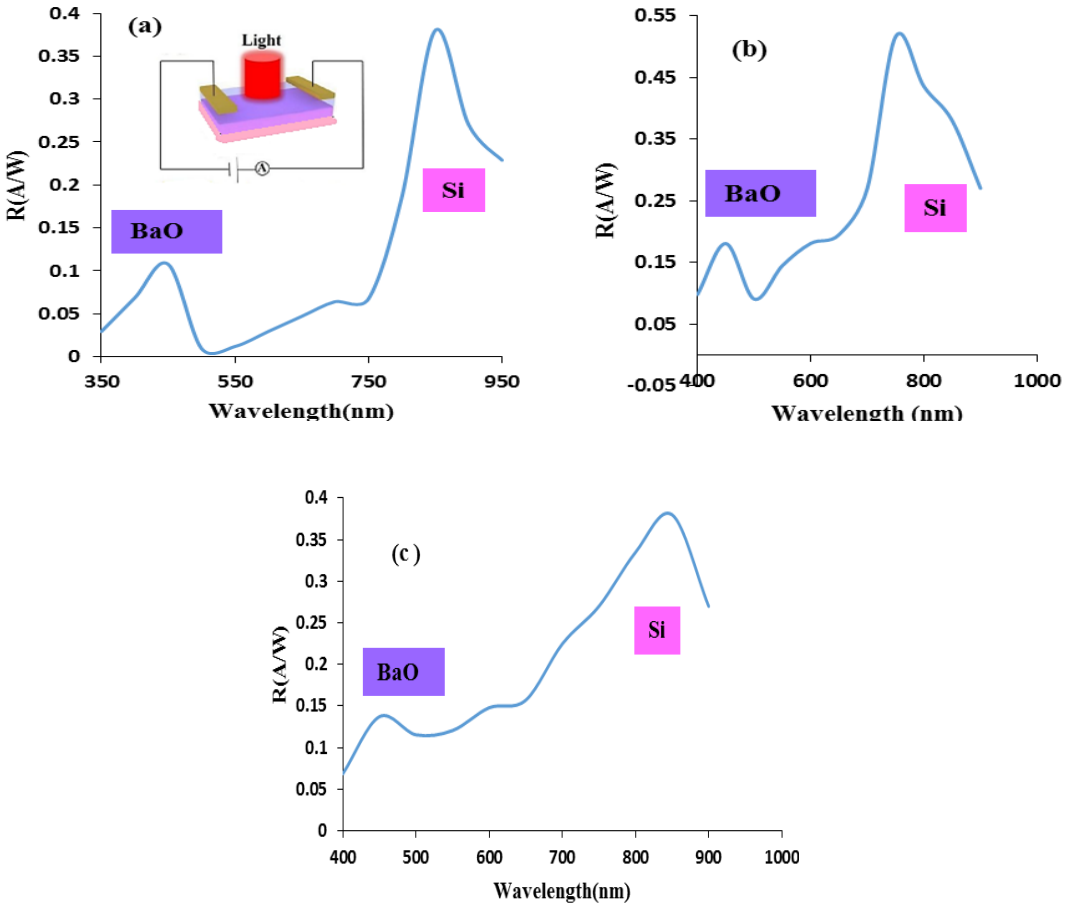

Fig. 7. Shows the spectral of responsivity (a) at 1M, (b) at 0.5 M and (c) at 0.25M.

(D*) detectivity can be determined using the formula (2) [32,33]:

$$D^*=R/(2eI_{dark}/S)^{1/2} \tag{2}$$

The effective surface area of the photodetector is denoted by S, the responsivity by R, the electron charge by e, and the dark current by I_{dark}. The photodetector (Ag/BaO/Si/Ag) exhibiting a calculated specific detectivity 1.5×10^{11}, 2.5×10^{12} and 1.9×10^{12} cm $Hz^{0.5}$ W^{-1} at wavelength 450nm at (1M, 0.5M and 0.25M) respectively as shown in figure 8.

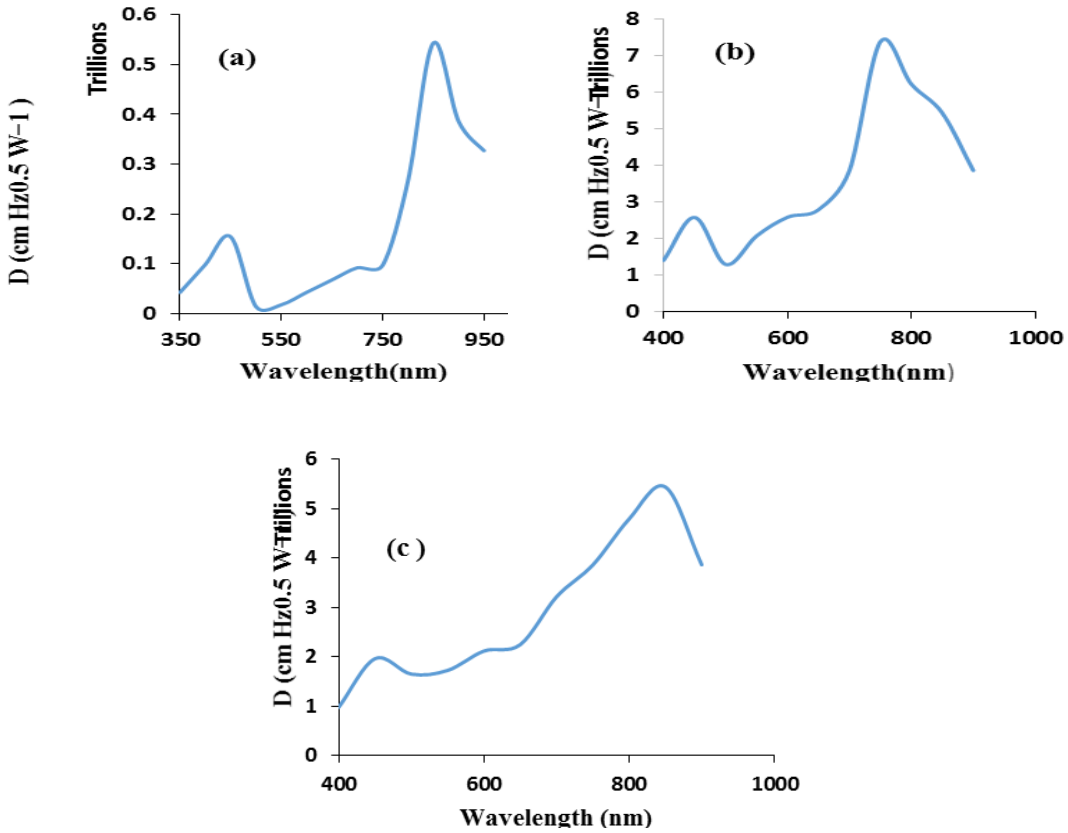

Fig. 8. Shows the spectral of detectivity (a) at 1M, (b) at 0.5 M and (c) at 0.25M.

The EQE, a crucial parameter in determining the number of electrons generated per incident photon, can be calculated as in equation(3):

$$EQE=Rhc/e\lambda \quad (3)$$

h is the Planck constant, λ is the excited wavelength, c is the light velocity, and e is the elementary electronic charge [31, 33] . Figure9 shows the quantum efficiency as function of wavelength for (Ag/BaO/Si/Ag) heterojunction with different molarity concentration (1M, 0.5M and 0.25M) The device shows high external quantum efficiency of 29% , 49% and 37% at a wavelength of 450 nm. While at 850 nm the quantum efficiency 55% and 85% and 55% respectively.

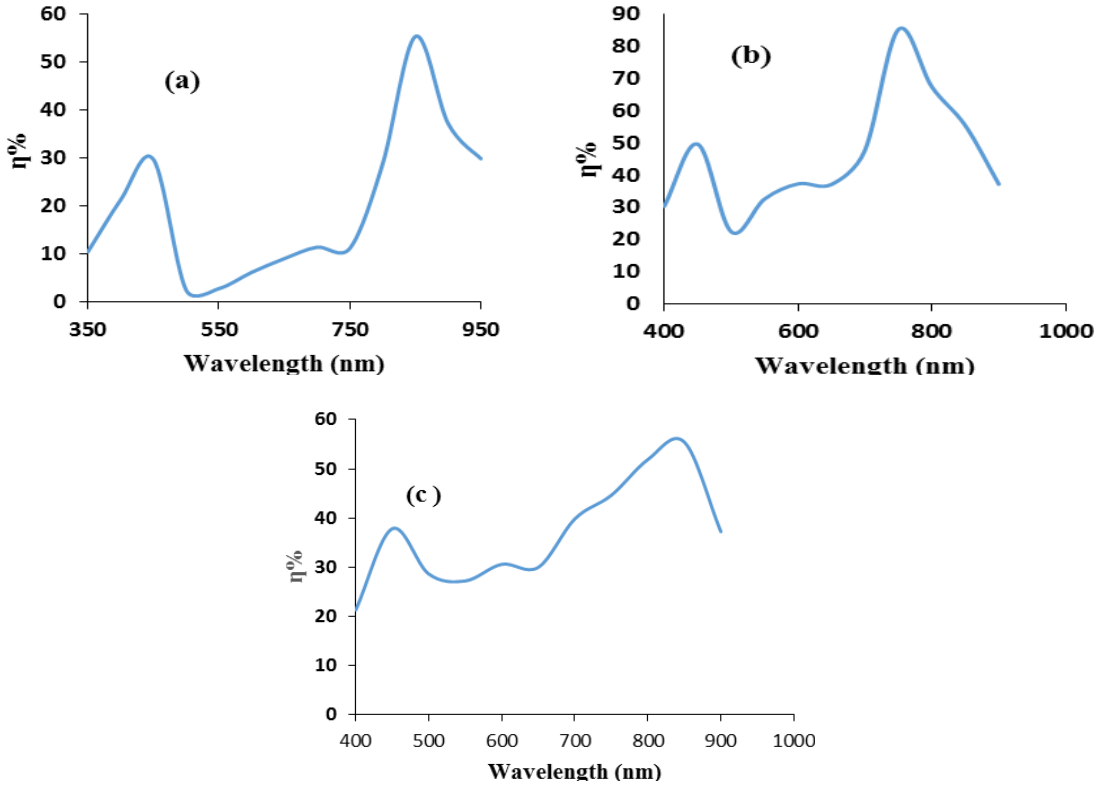

Fig. 9. Show the spectral of quantum efficiency (a) at 1M, (b) at 0.5 M and (c) at 0.25M.

4. Conclusion

Through the results obtained, we confirm our success in preparing Nan- barium oxide in an inexpensive way. We also succeeded in manufacturing a photodetector that has the highest response, detection, and quantitative efficiency at low concentrations because the material at high concentration tends to agglomerate, and thus defects are formed on the surface and the grain boundaries increase, Which increases the recombination process of electron –hole.

References

[1] Renukadevi R, Sundaram R, Kasinathan K., J of Nanostructures, 10: 67-76, 2020.

[2] Sundharam E, Jeevaraj AKS, Chinnusamy C, J Bionanoscience, 11(4):310-314, 2017; https://doi.org/10.1166/jbns.2017.1449

[3] Mousa AO, Nema NA, Hasan HH.m J Chem Pharm Res, 8:832-840, 2016

[4] E. Sundharam, A. Kingson Solomon Jeevaraj C. Chinnusamy, Journal of Bionanoscience, 11: 310-314, 2017; https://doi.org/10.1166/jbns.2017.1449

[5] S. Priscilla Prabhavathi, J. Punitha, P. Shameela Rajam, R. Ranjith, G. Suresh, N. Mala D. Maruthamuthu, Journal of Chemical and Pharmaceutical Research, 6(3):1472-1478, 2014.

[6] Cordoncillo E, Machado TR, Ferrazza L, Juanes D., EuroMed, 7616: 801-808, 2012; https://doi.org/10.1007/978-3-642-34234-9_85

[7] Zeenath Bazeera A, Irfana Amrin M, IOSR J Appl Phys, 3: 76-80, 2017; https://doi.org/10.9790/4861-17002017680

[8] Ahmad N, Wahab R, Alam M., J Nanosci Nanotechnol, 14: 5342-5348, 2014; https://doi.org/10.1166/jnn.2014.8852

[9] Devamani RHP, Alagar M., Asian Acad Res J Multidisciplinary 1, 60-75, 2014.

[10] R Renukadevi, R Sundaram, K Kasinathan, J Nanostruct, 10: pp. 67-76, 2020.

[11] D Maity and DC Agrawal, J Magn Magn Mater, Vol. 308, pp. 46-55, 2007;

https://doi.org/10.1016/j.jmmm.2006.05.001
[12] P Guardia, N Pérez, A Labarta, X Batlle, Langmuir, Vol. 26, pp. 5843-7, 2010; https://doi.org/10.1021/la903767e
[13] L Wang and M Muhammed, J Mater Chem, Vol. 9, pp. 2871-2879, 1999; https://doi.org/10.1039/a907098b
[14] M El-Hofy, A Salama, Defect and diffusion forum, 280: 1-8, 2008; https://doi.org/10.4028/www.scientific.net/DDF.280-281.1
[15] N Mohamed Basith, J Judith Vijaya, L John Kennedy, M Bououdina, Mater Sci Semiconduct Process, Vol. 17, pp. 110-18, 2014; https://doi.org/10.1016/j.mssp.2013.09.013
[16] Alia A. Shehab, Samir A. Maki, Ayad A. Salih, Ibn Al-Haitham Journal for Pure and Applied Sciences, 27(2): 158-169, 2014.
[17] Bushra K. Al-Maiyaly, Bushra H. Hussein, Ayad A. Salih, Auday H. Shaban, Shatha H. Mahdi, Iman H. Khudayer, AIP Conference Proceedings, 1968: 030046, (2018); https://doi.org/10.1063/1.5039233
[18] R Sankar, K Rizwana, KS Shivashangari, V Ravikumar, Appl Nanosci, Vol. 5, pp. 731-737, 2015; https://doi.org/10.1007/s13204-014-0369-3
[19] Majid H. Hassoni, Noor J. Sahib, Journal of Multidisciplinary Engineering Science Studies, 2(7): 725-732, 2016
[20] R. H. Athab, B. H. Hussein, Chalcogenide Letters, 20 (2), (2023) 91-100; https://doi.org/10.15251/CL.2023.202.91
[21] Falak Naz, Khalid Saeed, Applied Water Science, 12: 121- 132, 2022; https://doi.org/10.1007/s13201-022-01649-9
[22] Suresh G, Nirmala PN., Turk J Phys, 36: 392-7, 2012; https://doi.org/10.3906/fiz-1012-59
[23] Manauwar Ali Ansari, Nusrat Jahan, Materials Highlights Vol. 2(2): 23-28, 2021; https://doi.org/10.2991/mathi.k.210226.001
[24] Bahjat B. Kadhim, Imad H. Khaleel, Bushra H. Hussein, Kareem Ail Jasim, Auday H. Shaban, Bushra K.H. AL-Maiyaly, Shatha H. Mahdi, AIP Conference Proceedings, 1968: 030054, (2018); https://doi.org/10.1063/1.5039241
[25] Mahendra Kumar Trivedi, Rama Mohan Tallapragada, Alice Branton, Dahryn Trivedi, Omprakash Latiyal, Snehasis Jana, J Laser Opt Photonics, 2(2): 22-29, 2015; https://doi.org/10.4172/2469-410X.1000122
[26] R. H. Athab, B. H. Hussein, Chalcogenide Letters, 20 (7), (2023) 477-485; https://doi.org/10.15251/CL.2023.207.477
[27] Samir A. Maki, Alia A.A.Shehab, Ayad A. Salih, Ibn Al-Haitham Journal for Pure and Applied Sciences, 27(3): 279-290, 2014.
[28] Athab, R.H., Hussein, B.H., Digest Journal of Nanomaterials and Biostructures, 2022, 17(4), 1173 – 1180; https://doi.org/10.15251/DJNB.2022.174.1173
[29] Cui Y, Chen J, Zhang Y, Zhang X, Lei W, Di Y, et al., Appl Surf Sci, 396:1108-1120, 2017; https://doi.org/10.1016/j.apsusc.2016.11.095
[30] E Sundharam, AKS Jeevaraj, C Chinnusamy, J Bionanosci, Vol. 11, pp. 310-14, 2017; https://doi.org/10.1166/jbns.2017.1449
[31] MS Chauhan, R Kumar, A Umar, S Chauhan, G Kumar, M Faisal, et al., J Nanosci Nanotechnol, 11: 4061-6, 2011; https://doi.org/10.1166/jnn.2011.4166
[32] R Wahab, YS Kim, DS Lee, JM Seo, HS Shin, Sci Adv Mater, Vol. 2 , pp. 35-42, 2010; https://doi.org/10.1166/sam.2010.1064
[33] Hassanein K. Dakhil, Muneer H. J. Alzubaidy, Ahmed N. Abd, HIV Nursing; 23(3): 1699-1702, 2023.
[34] Estabrk Abd Latife, Ali Taher Mohi, Ahmed N. Abd, ACE Journal of Advance Research In Physical Science, 1(1): 5-11, 2023.